PHYSICAL REVIEW B **107**, L060501 (2023)

Letter

Metal borohydrides as ambient-pressure high-T_c superconductors

Simone Di Cataldo[1,2,*] and Lilia Boeri[1,3,†]
[1]*Dipartimento di Fisica, Sapienza Università di Roma, 00185 Rome, Italy*
[2]*Institute of Theoretical and Computational Physics, Graz University of Technology, NAWI Graz, 8010 Graz, Austria*
[3]*Centro Ricerche Enrico Fermi, Via Panisperna 89 A, 00184 Rome, Italy*

(Received 12 July 2022; revised 9 January 2023; accepted 24 January 2023; published 2 February 2023)

The extreme pressures required to stabilize the recently discovered *superhydrides* represent a major obstacle to their practical application. In this Letter, we propose and substantiate a route to attain high-temperature superconductivity in hydrides at ambient pressure, by doping commercial metal borohydrides. Using first-principles calculations based on density functional theory and Migdal-Eliashberg theory, we demonstrate that in $Ca(BH_4)_2$ a moderate hole doping of 0.03 holes per formula unit, obtained through a partial replacement of Ca with monovalent K, is sufficient to achieve T_c's as high as 110 K. The high T_c arises because of the strong electron-phonon coupling between the B-H σ molecular orbitals and bond-stretching phonons. Using a random sampling of large supercells to estimate the local effects of doping, we show that the required doping can be achieved without significant disruption of the electronic structure and at moderate energetic cost. Given the wide commercial availability of metal borohydrides, the ideas presented here can find prompt experimental confirmation. If successful, the synthesis of high-T_c doped borohydrides will represent a formidable advancement towards the technological exploitation of conventional superconductors.

DOI: 10.1103/PhysRevB.107.L060501

Since the discovery of superconductivity with a critical temperature (T_c) of 203 K at 150 GPa in H_3S [1,2], hydrogen-rich superconductors have revolutionized the landscape of superconductivity research. After H_3S, many other superhydrides with T_c's close to, or even above, room temperature have been found [3–12], but the extreme synthesis pressures represent an insurmountable obstacle to any practical application.

On the other hand, there exists an increasing demand for new materials enabling superconductor-based technologies: For most large-scale applications, synthesizability at ambient pressure is a strict requirement, whereas the threshold for T_c is sensibly lower than ambient temperature, but is dictated by the need to maintain a robust superconducting state under liquid nitrogen cooling [13].

The spectacular success of computational methods for superhydrides raises the hope that these techniques may accelerate the identification of suitable materials [14,15]. The first predictions which have started to appear in the literature follow essentially two different routes to lower the stabilization pressure within the conventional electron-phonon (*e*-*p*) scenario: (1) Optimization of the effective chemical pressure in ternary hydrides [16–20], through a careful combination of guest elements in host-guest metallic superhydrides; and (2) doping of nonhydride covalent structures [21–27], which exploits the large intrinsic *e*-*p* coupling of covalent insulators, turned metallic via either external or self-doping, as in B-doped diamond or MgB_2 [21,28–30].

Both approaches present potential drawbacks: While even the most optimized ternary hydrides seem to require a synthesis pressure of at least a few GPa [17], the T_c's of systems containing exclusively boron, carbon, and other heavier elements are unlikely to exceed the 80-K threshold found in the best-case scenarios [26,27], due to the intrinsic phonon energy scales determined by the relatively large boron and carbon atomic masses.

In this Letter we propose and substantiate an alternative, hybrid strategy which combines the best of both approaches, and could be possible to realize experimentally: Doping covalent bonds (ambient pressure) in a hydrogen-rich structure (higher T_c). In particular, we show, employing targeted first-principles calculations of the thermodynamical and superconducting properties, that metal borohydrides (MBH) can be turned into high-temperature conventional superconductors at ambient pressure, via small substitutional doping at the metal site, which effectively transforms MBH into highly tunable hole-doped hydrocarbons.

MBH form a broad class of materials widely used in commercial hydrogen storage applications, due to the high hydrogen content, and the ease of hydrogen uptake and dehydrogenation [31,32]. In these compounds boron and hydrogen form quasimolecular units arranged on open structures, with mono-, di-, or trivalent metals (M) on the interstitial sites. Our strategy to turn MBH into high-T_c superconductors is quite general, and consists in replacing a small fraction of M atoms with a lower-valence atom, realizing hole doping; in this work, we study the specific case of K doping of the α phase of $Ca(BH_4)_2$ [33].

Our calculations demonstrate that substitutional K doping in $Ca(BH_4)_2$ is energetically feasible up to at least 0.10

---

[*] simone.dicataldo@uniroma1.it
[†] lilia.boeri@uniroma1.it

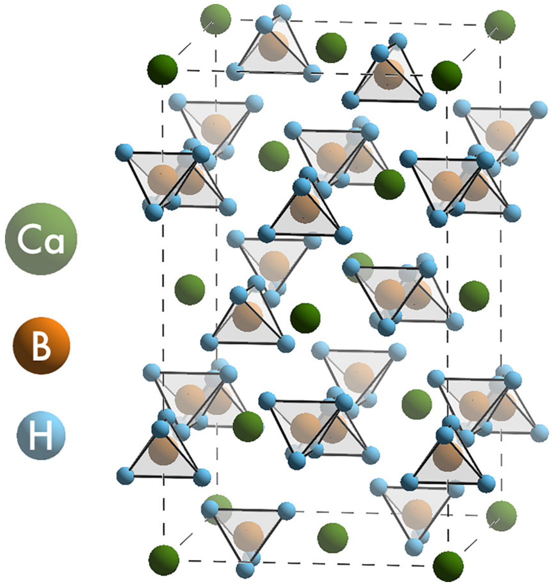

FIG. 1. Crystal structure of α-Ca(BH$_4$)$_2$. The Ca, B, and H atoms are shown as green, orange, and blue spheres, respectively. BH$_4{}^-$ anions are shown as tetrahedra.

h$^+$/f.u.; concentrations as low as 0.03 holes per formula unit (h$^+$/fu) are sufficient to induce superconductivity with a T_c as high as 110 K. As MBH are commercially available materials, we expect our work to find a broad audience of experimental researchers.

α-Ca(BH$_4$)$_2$ (Fig. 1) is a molecular crystal, in which boron and hydrogen form BH$_4$ tetrahedra, and Ca occupies interstitial sites. Ca is almost completely ionized (Ca^{++}), and donates charge to the BH$_4{}^-$ tetrahedra, which are thus not only isostructural, but also isoelectronic to methane (CH$_4$). The spacing between BH$_4{}^-$ molecular units is quite large, about 3.5 Å, indicating extremely weak intermolecular interactions.

Figure 2 shows the electronic band structure and the atom-projected density of states (DOS) of the α phase of Ca(BH$_4$)$_2$. Undoped α-Ca(BH$_4$)$_2$ is an insulator, with a calculated direct band gap of 5 eV. The bands have a reduced dispersion, as is typical of molecular crystals; the electronic DOS exhibits extremely sharp and narrow peaks, particularly near the valence band maximum (VBM). Electronic states in this region have a mixed (50/50) B/H character and derive from the threefold degenerate $1t_2$ (0 to -2 eV) and the single $2a_1$ (-6 to -8 eV) molecular σ orbitals of BH$_4$, which are expected to couple strongly to B-H bond-stretching and bond-bending phonons.

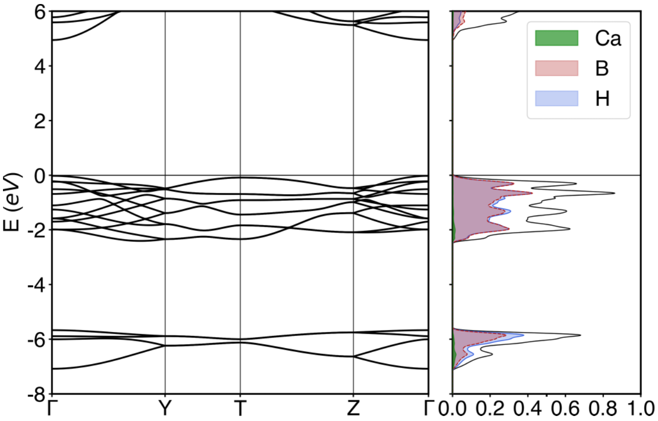

FIG. 2. Electronic band structure and atom-projected DOS of Ca(BH$_4$)$_2$. The energy zero is set to the valence band maximum. The DOS is in units of states eV^{-1} atom^{-1}.

Due to the extremely sharp profile of the DOS, even extremely small hole dopings are sufficient to shift the Fermi energy into the large DOS, large *e-p* region below the VBM, which should induce high-T_c conventional superconductivity (SC).

Hole doping in Ca(BH$_4$)$_2$ can be realized by substituting Ca with a monovalent atom. In this work, we consider K, which is the neighbor of Ca in the periodic table, and hence has a very similar size and core. Replacing a fraction δ of divalent Ca with monovalent K amounts to doping α-Ca(BH$_4$)$_2$ with δ holes/f.u.; in an ideal rigid-band picture, these holes would form at the top of the valence band, turning K-doped Ca(BH$_4$)$_2$ into a self-doped version of methane (CH$_4$).

Due to the presence of stiff covalent bonds coupled by symmetry to bond-stretching phonons, doped hydrocarbons have long been postulated to exhibit large *e-p* coupling; controversial reports of high-T_c superconductivity in polyacenes doped with alkali and alkaline earths (*electron* doping) have appeared in the early 2010s [34–37]. However, doping hydrocarbons and related C-H systems with *holes* has so far proven impossible, as intercalation with electronegative elements (I, F, Cl) is ineffective, and doping the C-H sublattice by substitutional atoms or vacancies is extremely unfavorable energetically and tends to seriously disrupt the crystal and electronic structure due to the presence of stiff covalent bonds [38,39].

In K-doped Ca(BH$_4$)$_2$, on the other hand, doping only involves the metal site, which is very weakly bonded to the rest of the structure. This should allow a convenient fine-tuning of the superconducting properties at a reasonable energy cost, without major modifications of the structure [40].

To substantiate our hypotheses, we computed the superconducting properties of K-doped Ca(BH$_4$)$_2$ for various hole concentrations δ, computing the isotropic Eliashberg functions for various values of δ using density functional perturbation theory [41], and obtaining the T_c by numerically solving the isotropic Eliashberg equations, assuming a value of the Morel-Anderson pseudopotential of 0.10 [42].

Doping is simulated using the virtual crystal approximation (VCA), which amounts to replacing each Ca (pseudo)atom in the α-Ca(BH$_4$)$_2$ structure with an average virtual (pseudo)atom, obtained by mixing K and Ca in the appropriate proportions.

In Fig. 3 we report a summary of the electronic and superconducting properties of K-doped Ca(BH$_4$)$_2$ as a function of the hole concentration δ. The DOS at the Fermi level N_{E_F} [Fig. 3(a)] rapidly increases with doping, as does the total *e-p* coupling constant λ [Fig. 3(c)], while the average phonon frequency $\omega_{\log}$ [Fig. 3(b)] slightly decreases. In the Eliashberg function (shown in Fig. S2 of the Supplemental Material [43]) almost all *e-p* coupling is concentrated in the high-energy B-H stretching and bending modes. For δ larger than 0.10

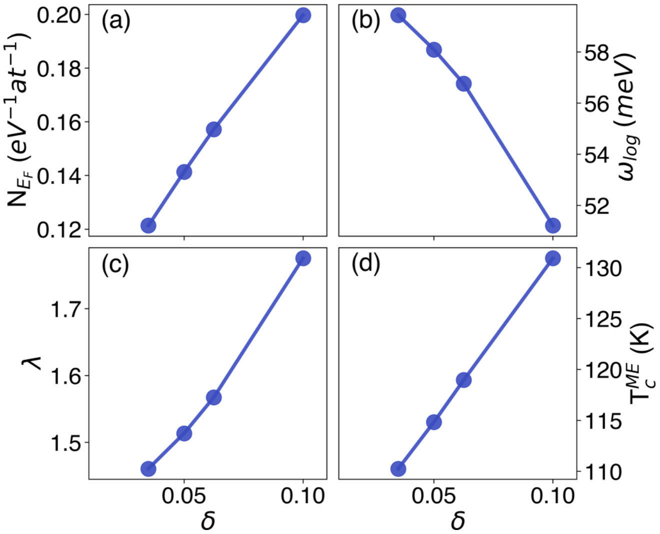

FIG. 3. Electronic and superconducting properties as a function of the doping δ. (a) DOS at the Fermi level. (b) Logarithmic average phonon frequency $\omega_{\log}$. (c) *e-p* coupling coefficient λ. (d) Superconducting critical temperature T_c.

the system develops a dynamical instability, while for values smaller than 0.03 the Fermi energy is too close to the VBM to allow a reasonable estimate of λ and T_c. T_c attains its maximum value of 130 K at $\delta = 0.10$ and decreases linearly with decreasing δ down to 110 K at $\delta = 0.03$; extrapolating this trend, we can reasonably suppose that T_c's higher than 100 K may be achieved for dopings $\delta \gtrsim 0.01$.

The VCA has the advantage of making T_c calculations feasible even for small dopings, correctly capturing the average effect of substitutional doping on the electronic structure, in particular the critical role of electronic screening on phonon spectra and *e-p* matrix elements [37]. However, effects such as charge localization, deep defect levels, or carrier trapping [24,44], which may sensibly affect the electronic structure, require more complex approximations that can capture the local environment of the impurities.

To simulate these effects, we developed an *ad hoc* scheme, based on averaging over random supercells. First, we constructed a $2\times2\times2$ supercell containing 32 formula units of $Ca(BH_4)_2$ (352 atoms); then, to simulate hole concentrations from $\delta = 0.03$ to $\delta = 0.5$, we substituted Ca atoms with the appropriate fraction of K, placed at random positions; for each value of δ, we generated ten supercells. These supercells were then relaxed to minimize stress and forces, before computing the total energies and DOS (Fig. 4). Computations on the supercells were performed using the Vienna *ab initio* simulation package (VASP). Further details are provided in the Supplemental Material (SM) [43]. The average DOS for each doping was then obtained by performing a weighted average over the relative supercells, with weights corresponding to the probability of that configuration (see SM for further details [43]). The average DOS for different values of δ are shown in Fig. 4. Although doping causes sizable modifications of the DOS for $\delta > 0.12$, especially in the low-lying region below −6 eV, the DOS for δ up to 0.09 are essentially unchanged compared to the undoped compound. In particular, there are no intergap states up to $\delta = 0.09$, and the relative weight remains negligible up to $\delta = 0.25$.

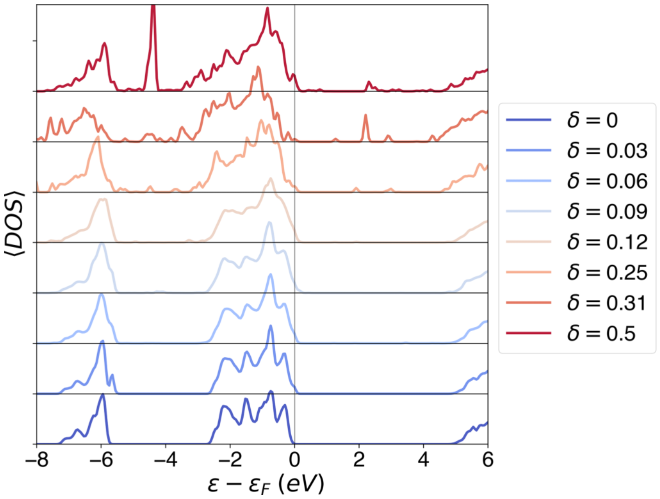

FIG. 4. Density of states (DOS) of K-doped $Ca(BH_4)_2$ as a function of the hole concentration δ. The Fermi energy is taken as energy zero except for $\delta = 0$, in which the VBM is used.

Hence, for doping of interest the main effect of K/Ca substitution is indeed a quasirigid shift of the Fermi level into the valence band, well reproduced by VCA; in particular, the states just below the VBM, which participate in the SC pairing, are only weakly influenced by doping. This is expected, since σ orbitals of the BH_4^- molecular ions are only weakly affected by distortions and rearrangements of atoms in the crystal structure which do not modify the overall shape of the molecular ion itself.

Using supercells we can also estimate the energetic cost of K substitution into the Ca site. In Fig. 5 we show the formation energy of $K_\delta Ca_{1-\delta}(BH_4)_2$ with respect to decomposition into $K+Ca(BH_4)_2$ [45], for all configurations sampled (ten for

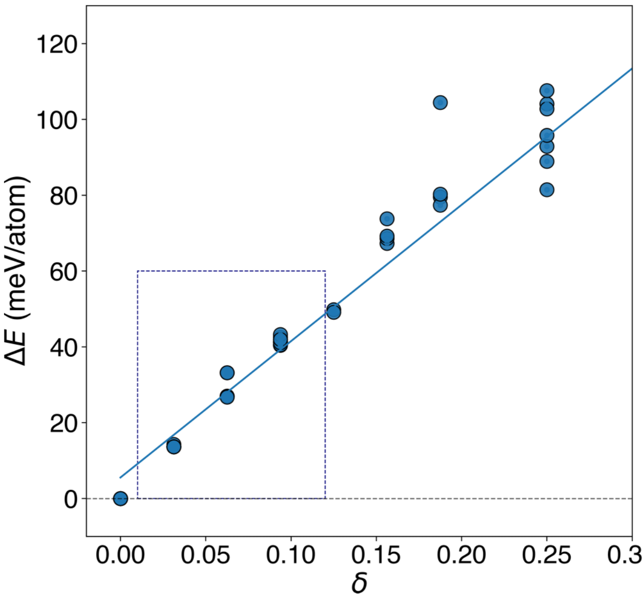

FIG. 5. Formation energy ΔE as a function of hole doping δ.

each doping). The formation energies δE increase linearly with doping, with little dispersion for different supercells, remaining well below 150 meV/atom.

On purely energetic grounds, these values indicate that K doping of $Ca(BH_4)_2$ should be experimentally feasible. However, experimental synthesis conditions depend on complex details of the kinetic barrier protecting the doped structure from decomposition, and on the entropy contribution to the free energy, whose evaluation goes well beyond the scope of this Letter.

Moreover, independently of their energetic cost, not all perturbations induced by doping will have the same effect on superconductivity; while small distortions and rearrangements of BH_4^- anions within the open α structure should have only minor effects on the superconducting properties, dehydrogenation, which implies a breaking of B-H bonds, has severe consequences, since it implies a major rearrangement of the whole electronic structure. We will therefore assume that the dehydrogenation energy can be used to estimate an effective synthesizabilty threshold for K-doped $Ca(BH_4)_2$.

A hand-waving estimate can be obtained as follows. Assuming the measured dehydrogenation temperature of $Ca(BH_4)_2$, which is around 700 K [46–48], to be a reasonable guess of the kinetic barrier for dehydrogenation, doped $Ca(BH_4)_2$ should be able to withstand perturbations with a positive ΔE of the order of 60 meV/atom without decomposing. This corresponds to a doping of $\delta \sim 10$ (Fig. 5), which, as Fig. 3(d) shows, largely exceeds the doping levels required for high-T_c superconductivity. Hence, high-T_c superconductivity should be observable, before dehydrogenation sets in.

In summary, in this Letter we proposed a strategy to attain high-T_c conventional superconductivity in the complex bordohydride $Ca(BH_4)_2$ using substitutional doping of monovalent K on the Ca site, and substantiated it with first-principles calculations.

K-doped $Ca(BH_4)_2$ behaves essentially as hole-doped methane (CH_4), where the high T_c derives from a strong coupling between σ bonding electronic states and bond-stretching phonons of the BH_4^- molecular units. Compared to CH_4, however, the big advantage of $Ca(BH_4)_2$ is that hole doping is realized by acting on the weakly bonded metal site, and not on the covalent B-H (or C-H) sublattice, and this causes only minor disruptions of the crystal and electronic structure, implying an affordable energy cost. According to our calculations, a partial replacement of 3% Ca atoms with K atoms would have an energy cost of around 50 meV/atom, which is below the dehydrogenation threshold, and lead to an estimated T_c of 110 K at ambient pressure, almost on par with the best copper-oxide superconductors. With a figure of merit S between 2.8 and 3.3 [13], doped $Ca(BH_4)_2$ is better than any other superhydride, as well as all other known ambient-pressure conventional superconductors ($S = 1$ in MgB_2), and very close to HgBaCaCuO.

Note that the strategy proposed here is very general, and can in principle be applied to turn any of the many existing MBH into doped hydrocarbons, by suitable metal substitutions. We would like to stress that unlike other proposed hydrogenated covalent superconductors based on hypothetical two-dimensional systems [38,49], doped MBH is a bulk superconductor obtained from doping an existing compound. Moreover, our calculations indicate that K doping is thermodynamically feasible. We are strongly convinced that, if synthesized, doped MBH will represent a huge leap forward in research on high-temperature superconductors.

Given the easy commercial availability of metal borohydrides, we hope that our work will stimulate a positive response from experimentalists.

The authors warmly thank A. Sanna for sharing the code to solve the isotropic Eliashberg equations. L.B. and S.D.C. acknowledge funding from the Austrian Science Fund (FWF) Grant No. P30269-N36 and support from Fondo Ateneo-Sapienza 2017-2020. S.D.C. acknowledges computational resources from CINECA, Projects No. IsC90-HTS-TECH and No. IsC99-ACME-C, and the Vienna Scientific Cluster, Project No. 71754 “TEST.”

[1] A. P. Drodzov, M. I. Eremets, I. A. Troyan, V. Ksenofontov, and S. I. Shylin, Conventional superconductivity at 203 Kelvin at high pressures in the sulfur hydride system, Nature (London) **525**, 73 (2015).

[2] M. Einaga, M. Sakata, T. Ishikawa, K. Shimizu, M. Eremets, A. P. Drodzov, I. A. Troyan, N. Hirao, and Y. Ohishi, Crystal structure of the superconducting phase of sulfur hydride, Nat. Phys. **12**, 835 (2016).

[3] H. Liu, I. I. Haumov, Z. M. Geballe, M. Somayazulu, J. S. Tse, and R. J. Hemley, Dynamics and superconductivity in compressed lanthanum superhydride, Phys. Rev. B **98**, 100102(R) (2018).

[4] M. Somayazulu, M. Ahart, A. K. Mishra, Z. M. Geballe, M. Baldini, Y. Meng, V. V. Struzhkin, and R. J. Hemley, Evidence for Superconductivity above 260 K in Lanthanum Superhydride at Megabar Pressures, Phys. Rev. Lett. **122**, 027001 (2019).

[5] A. P. Drodzov, P. P. Kong, S. P. Besedin, M. A. Kuzonikov, S. Mozaffari, L. Balicas, F. F. Balakirev, D. E. Graf, V. B. Prakapenka, E. Greenberg, D. A. Knyazev, M. Tkacz, and M. I. Eremets, Superconductivity at 250 K in lanthanum hydride under high pressure, Nature (London) **569**, 528 (2019).

[6] E. Snider, N. Dasenbrock-Gammon, R. McBride, M. Debessai, H. Vindana, K. Vencatasamy, K. V. Lawler, A. Salamat, and R. P. Dias, Room-temperature superconductivity in a carbonaceous sulfur hydride, Nature (London) **586**, 373 (2020).

[7] L. Ma, K. Wang, Y. Xie, X. Yang, Y. Wang, M. Zhou, H. Liu, X. Yu, Y. Zhao, H. Wang, G. Liu, and Y. Ma, High-Temperature Superconducting Phase in Clathrate Calcium Hydride CaH_6 up to 215 K at a Pressure of 172 GPa, Phys. Rev. Lett. **128**, 167001 (2022).

[8] D. V. Semenok, A. G. Kvashin, A. G. Ivanova, V. Svitlyk, V. Y. Fominski, A. V. Sadakov, O. A. Sobolevskiy, V. M. Pudalov, I. A. Troyan, and A. R. Oganov, Superconductivity at 161 K in

thorium hydride ThH_{10}: Synthesis and properties, Mater. Today **33**, 36 (2020).

[9] P. Kong, V. S. Minkov, M. A. Kuzovnikov, A. P. Drodzov, S. P. Besedin, S. Mozaffari, L. Balicas, F. F. Balekirev, V. B. Prakapenka, S. Chariton, D. V. Semenok, E. Greenberg, and M. I. Eremets, Superconductivity up to 243 K in the yttrium-hydrogen system under high pressure, Nat. Commun. **12**, 5075 (2021).

[10] I. A. Troyan, D. V. Semenok, A. G. Kvashin, A. V. Sadakov, O. A. Sobolevskiy, V. M. Pudalov, A. G. Ivanova, V. B. Prakapenka, E. Greenberg, A. G. Gavriliuk, V. V. Struzhkin, A. Bergara, I. Errea, R. Bianco, M. Calandra, F. Mauri, L. Monacelli, R. Akashi, and A. R. Oganov, Anomalous high-temperature superconductivity in YH_6, Adv. Mater. **33**, 2006832 (2021).

[11] W. Chen, D. V. Semenok, X. Huang, H. Shu, X. Li, D. Duan, T. Cui, and A. R. Oganov, High-Temperature Superconducting Phases in Cerium Superhydride with a T_c up to 115 K Below a Pressure of 1 Megabar, Phys. Rev. Lett. **127**, 117001 (2021).

[12] A. D. Grockowiak, M. Ahart, T. Helm, W. A. Coniglio, R. Kumar, K. Glazyrin, G. Garbarino, Y. Meng, M. Oliff, V. Williams, N. W. Ashcroft, R. J. Hemley, M. Somayazulu, and S. W. Tozer, Hot hydride superconductivity above 550 K, Front. Electron. Mater. **2**, 837651 (2022).

[13] C. J. Pickard, I. Errea, and M. Eremets, Superconducting hydrides under pressure, Annu. Rev. Condens. Matter Phys. **11**, 57 (2020).

[14] L. Boeri and G. B. Bachelet, Viewpoint: The road to room-temperature conventional superconductivity, J. Phys.: Condens. Matter **31**, 234002 (2019).

[15] J. A. Flores-Livas, L. Boeri, A. Sanna, G. Profeta, R. Arita, and M. Eremets, A perspective on conventional high-temperature superconductors at high pressure: Methods and materials, Phys. Rep. **856**, 1 (2020).

[16] S. Di Cataldo, C. Heil, W. von der Linden, and L. Boeri, $LaBH_8$: Towards high-T_c low-pressure superconductivity in ternary superhydrides, Phys. Rev. B **104**, L020511 (2021).

[17] R. Lucrezi, S. Di Cataldo, W. von der Linden, L. Boeri, and C. Heil, In-silico synthesis of lowest-pressure high-T_c ternary superhydrides, npj Comput. Mater. **8**, 119 (2022).

[18] S. Di Cataldo, W. von der Linden, and L. Boeri, Phase diagram and superconductivity of calcium borohydrides at extreme pressures, Phys. Rev. B **102**, 014516 (2020).

[19] Z. Zhang, T. Cui, M. J. Hutcheon, A. M. Shipley, H. Song, M. Du, V. Z. Kresin, D. Duan, C. J. Pickard, and Y. Yao, Design Principles for High Temperature Superconductors with Hydrogen-Based Alloy Backbone at Moderate Pressure, Phys. Rev. Lett. **128**, 047001 (2022).

[20] K. P. Hilleke and E. Zurek, Rational Design of Superconducting Metal Hydrides via Chemical Pressure Tuning, Angewandte Chemie **61**, e202207589 (2022).

[21] E. A. Ekimov, V. A. Sidorov, E. D. Bauer, N. N. Mel'nik, N. J. Curro, J. D. Thompson, and S. M. Stishov, Superconductivity in diamond, Nature (London) **428**, 542 (2004).

[22] V. A. Sidorov and E. A. Ekimov, Superconductivity in diamond, Diam. Relat. Mater. **19**, 351 (2010).

[23] X. Cui, K. P. Hilleke, X. Wang, M. Lu, M. Zhang, E. Zurek, W. Li, D. Zhang, Y. Yan, and T. Bi, RbB_3Si_3: An alkali metal borosilicide that is metastable and superconducting at 1 atm, J. Phys. Chem. C **124**, 14826 (2020).

[24] J. A. Flores-Livas, A. Sanna, M. Grauzinyte, A. Davydov, S. Goedecker, and M. A. L. Marques, Emergence of superconductivity in doped H_2O ice at high pressure, Sci. Rep. **7**, 6825 (2017).

[25] H. Rosner, A. Kitaigorodsky, and W. E. Pickett, Prediction of High T_c Superconductivity in Hole-Doped LiBC, Phys. Rev. Lett. **88**, 127001 (2002).

[26] S. Saha, S. D. Cataldo, M. Amsler, W. von der Linden, and L. Boeri, High-temperature conventional superconductivity in the boron-carbon system: Material trends, Phys. Rev. B **102**, 024519 (2020).

[27] S. Di Cataldo, S. Qulaghasi, G. B. Bachelet, and L. Boeri, High-T_c superconductivity in doped boron-carbon clathrates, Phys. Rev. B **105**, 064516 (2022).

[28] J. Kortus, I. I. Mazin, K. D. Belashchenko, V. P. Antropov, and L. L. Boyer, Superconductivity of Metallic Boron in MgB_2, Phys. Rev. Lett. **86**, 4656 (2001).

[29] L. Boeri, J. Kortus, and O. K. Andersen, Three-Dimensional MgB_2-Type Superconductivity in Hole-Doped Diamond, Phys. Rev. Lett. **93**, 237002 (2004).

[30] T. A. Strobel and L. Zhu, Abstract S24.00003: Superconductivity in carbon-boron clathrates, APS Match Meeting, 2022, https://meetings.aps.org/Meeting/MAR22/Session/S24.3.

[31] S. ichi Orimo, Y. Nakamori, J. R. Eliseo, A. Züttel, and C. M. Jensen, Complex hydrides for hydrogen storage, Chem. Rev. **107**, 4111 (2007).

[32] S.-W. Li, Y. Yan, S.-I. Orimo, A. Züttel, and C. M. Jensen, Recent progress in metal borohydrides for hydrogen storage, Energies **4**, 185 (2011).

[33] Y. Filinchuk, E. Rönnebro, and D. Chandra, Crystal structures and phase transformations in $Ca(BH_4)_2$, Acta Mater. **57**, 732 (2009).

[34] A. Devos and M. Lannoo, Electron-phonon coupling for aromatic molecular crystals: Possible consequences for their superconductivity, Phys. Rev. B **58**, 8236 (1998).

[35] R. Mitsuhashi, Y. Suzuki, Y. Yamanari, H. Mitamura, T. Kambe, N. Ikeda, H. Okamoto, A. Fujiwara, M. Yamaji, N. Kawasaki, Y. Maniwa, and Y. Kubozono, Superconductivity in alkali-metal-doped picene, Nature (London) **464**, 76 (2010).

[36] A. Subedi and L. Boeri, Vibrational spectrum and electron-phonon coupling of doped solid picene from first principles, Phys. Rev. B **84**, 020508(R) (2011).

[37] M. Casula, M. Calandra, and F. Mauri, Local and nonlocal electron-phonon couplings in K_3 picene and the effect of metallic screening, Phys. Rev. B **86**, 075445 (2012).

[38] G. Savini, A. C. Ferrari, and F. Giustino, First-Principles Prediction of Doped Graphane as a High-Temperature Electron-Phonon Superconductor, Phys. Rev. Lett. **105**, 037002 (2010).

[39] J. A. Flores-Livas, M. Grauzinyte, L. Boeri, G. Profeta, and A. Sanna, Superconductivity in doped polyethylene at high pressure, Eur. Phys. J. B **91**, 176 (2018).

[40] J. E. Moussa and M. L. Cohen, Using molecular fragments to estimate electron-phonon coupling and possible superconductivity in covalent materials, Phys. Rev. B **78**, 064502 (2008).

[41] S. Baroni, S. de Gironcoli, A. D. Corso, and P. Giannozzi, Phonons and related crystal properties from density-functional perturbation theory, Rev. Mod. Phys. **73**, 515 (2001).

[42] Calculations were performed using DFPT as implemented in QUANTUM ESPRESSO. Integration of electron-phonon properties

was performed on 3×3×3 grid for phonons and 16×16×16 grid for electrons, using a Gaussian smearing of 200 meV. Further computational details are provided in the Supplemental Material [41,43,50–54].

[43] See Supplemental Material at http://link.aps.org/supplemental/10.1103/PhysRevB.107.L060501 for further details on the structural, electronic, and vibrational properties of the doped phases, as well as additional computational details on the simulation of the doped supercells and the calculations of vibrational and superconducting properties.

[44] C. Freysoldt, B. Grabowski, T. Hickel, J. Neugebauer, G. Kresse, A. Janotti, and C. G. Van de Walle, First-principles calculations for point defects in solids, Rev. Mod. Phys. **86**, 253 (2014).

[45] For Ca and K we assumed a face-centered- and a body-centered-cubic structure, respectively. The formation energy was computed as described in Ref. [44] for a neutral defect.

[46] M. D. Riktor, M. H. Sorby, K. Chlopek, M. Fichtner, F. Buchter, A. Züttel, and B. C. Hauback, *In situ* synchrotron diffraction studies of phase transitions and thermal decomposition of $Mg(BH_4)_2$ and $Ca(BH_4)_2$, J. Mater. Chem. **17**, 4939 (2007).

[47] J.-H. Kim, S.-A. Jin, J.-H. Shim, and Y. W. Cho, Thermal decomposition behavior of calcium borohydride $Ca(BH_4)_2$, J. Alloys Compd. **461**, L20 (2008).

[48] C. J. Sahle, C. Sternemann, C. Giacobbe, Y. Yan, C. Weis, M. Harder, Y. Forov, G. Spiekermann, M. Tolan, M. Krisch, and A. Remhof, Formation of CaB_6 in the thermal decomposition of the hydrogen storage material $Ca(BH_4)_2$, Phys. Chem. Chem. Phys. **18**, 19866 (2016).

[49] J. Bekaert, M. Petrov, A. Aperis, P. M. Oppeneer, and M. V. Milosevic, Hydrogen-Induced High-Temperature Superconductivity in Two-Dimensional Materials: The Example of Hydrogenated Monolayer MgB_2, Phys. Rev. Lett. **123**, 077001 (2019).

[50] G. Kresse and J. Furthmüller, Efficient iterative schemes for *ab initio* total-energy calculations using a plane-wave basis set, Phys. Rev. B **54**, 11169 (1996).

[51] K. Momma and F. Izumi, VESTA: A three-dimensional visualization system for electronic and structural analysis, J. Appl. Cryst. **41**, 653 (2008).

[52] P. Giannozzi, S. Baroni, N. Bonini, M. Calandra, R. Car, C. Cavazzoni, D. Ceresoli, G. L. Chiarotti, M. Cococcioni, and I. Dabo, QUANTUM ESPRESSO: A modular and open-source software project for quantum simulation of materials, J. Phys.: Condens. Matter **21**, 395502 (2009).

[53] P. Giannozzi, O. Andreussi, T. Brumme, O. Bunau, M. B. Nardelli, M. Calandra, R. Car, C. Cavazzoni, D. Ceresoli, M. Cococcioni, N. Colonna, I. Carnimeo, A. D. Corso, S. de Gironcoli, P. Delugas, R. A. DiStasio, A. Ferretti, A. Floris, G. Fratesi, G. Fugallo *et al.*, Advanced capabilities for materials modelling with quantum espresso, J. Phys.: Condens. Matter **29**, 465901 (2017).

[54] D. R. Hamann, Optimized norm-conserving Vanderbilt pseudopotentials, Phys. Rev. B **88**, 085117 (2013).